



## Article

# Assessing the Sensitivity of Vegetation Cover to Climate Change in the Yarlung Zangbo River Basin Using Machine Learning Algorithms

Lizhuang Cui <sup>1,2</sup> , Bo Pang <sup>1,2,\*</sup>, Gang Zhao <sup>1,2,3</sup> , Chunguang Ban <sup>1,2</sup>, Meifang Ren <sup>4,5</sup>, Dingzhi Peng <sup>1,2</sup> , Depeng Zuo <sup>1,2</sup> and Zhongfan Zhu <sup>1,2</sup>

- <sup>1</sup> College of Water Sciences, Beijing Normal University, Beijing 100875, China; cuilizhuang@mail.bnu.edu.cn (L.C.); gang.zhao@bristol.ac.uk (G.Z.); banchunguang@mail.bnu.edu.cn (C.B.); dzpeng@bnu.edu.cn (D.P.); dpzuo@bnu.edu.cn (D.Z.); zhuzhongfan1985@bnu.edu.cn (Z.Z.)
- <sup>2</sup> Beijing Key Laboratory of Urban Hydrological Cycle and Sponge City Technology, College of Water Sciences, Beijing Normal University, Beijing 100875, China
- <sup>3</sup> School of Geographical Science, University of Bristol, Bristol BS8 1SS, UK
- <sup>4</sup> China Academy of Urban Planning & Design, Beijing 100044, China; renmeifang@mail.bnu.edu.cn
- <sup>5</sup> Department of Hydraulic Engineering, Tsinghua University, Beijing 100084, China
- \* Correspondence: pb@bnu.edu.cn

**Abstract:** Vegetation is a key indicator of the health of most terrestrial ecosystems and different types of vegetation exhibit different sensitivity to climate change. The Yarlung Zangbo River Basin (YZRB) is one of the highest basins in the world and has a wide variety of vegetation types because of its complex topographic and climatic conditions. In this paper, the sensitivity to climate change for different vegetation types, as reflected by the Normalized Difference Vegetation Index (NDVI), was assessed in the YZRB. Three machine learning models, including multiple linear regression, support vector machine, and random forest, were adopted to simulate the response of each vegetation type to climatic variables. We selected random forest, which showed the highest performance in both the calibration and validation periods, to assess the sensitivity of the NDVI to temperature and precipitation changes on an annual and monthly scale using hypothetical climatic scenarios. The results indicated there were positive responses of the NDVI to temperature and precipitation changes, and the NDVI was more sensitive to temperature than to precipitation on an annual scale. The NDVI was predicted to increase by 1.60–4.68% when the temperature increased by 1.5 °C, while it only changed by 0.06–0.24% when the precipitation increased by 10% in the YZRB. Monthly, the vegetation was more sensitive to temperature changes in spring and summer. Spatially, the vegetation was more sensitive to temperature increases in the upper and middle reaches, where the existing temperatures were cooler. The time-lag effects of climate were also analyzed in detail. For both temperature and precipitation, Needleleaf Forest and Broadleaf Forest had longer time lags than those of other vegetation types. These findings are useful for understanding the eco-hydrological processes of the Tibetan Plateau.

**Keywords:** vegetation response; attribution analysis; machine learning; NDVI; the Yarlung Zangbo River Basin



**Citation:** Cui, L.; Pang, B.; Zhao, G.; Ban, C.; Ren, M.; Peng, D.; Zuo, D.; Zhu, Z. Assessing the Sensitivity of Vegetation Cover to Climate Change in the Yarlung Zangbo River Basin Using Machine Learning Algorithms. *Remote Sens.* **2022**, *14*, 1556. <https://doi.org/10.3390/rs14071556>

Academic Editors: Pingping Luo, Xindong Wei, Kanhua Yu, Bin Guo and Joshua Viers

Received: 4 February 2022

Accepted: 14 March 2022

Published: 23 March 2022

**Publisher's Note:** MDPI stays neutral with regard to jurisdictional claims in published maps and institutional affiliations.



**Copyright:** © 2022 by the authors. Licensee MDPI, Basel, Switzerland. This article is an open access article distributed under the terms and conditions of the Creative Commons Attribution (CC BY) license (<https://creativecommons.org/licenses/by/4.0/>).

## 1. Introduction

The sensitivity to climate change for different vegetation types in terrestrial ecosystems can have important feedback on hydrology, climate, and ecology [1–4]. Owing to the spatial heterogeneity, vegetation's response to climate change varies greatly, with different temporal responses and spatial patterns [5]. Given the importance of identifying ecologically sensitive areas for land planning and water resource management, it is essential to identify and then prioritize vegetation that is sensitive to climate change, especially in ecologically fragile regions such as the Tibetan Plateau [6–8].

The sensitivity of vegetation to climate change is the focus of global climate change and terrestrial ecosystem research [9–11]. A variety of dynamic and statistical models have been developed to explore the response of vegetation to climate change [12]. Dynamic models, including the Lund-Potsdam-Jena Model [13,14] and the Sheffield Dynamic Global Vegetation Model [15], can simulate dynamic ecosystem processes and provide information on spatiotemporal changes in vegetation under climate change [16–18]. However, data availability often restricts the application of dynamic models, especially for data-scarce regions [19]. Statistical models, which simulate the relationship between vegetation indices, such as the Normalized Difference Vegetation Index (NDVI) [20], Net Primary Productivity (NPP) [21], Enhanced Vegetation Index (EVI) [9], Leaf Area Index (LAI) [22], and climatic variables, have been valuable supplements for dynamic models in many application scenarios [23,24]. The most popular regression equation models—the machine learning models—have attracted widespread interest from researchers owing to their advantages in simulating complex nonlinear systems and their ability to handle multi-dimensional and multi-variety data [10,25,26].

The Yarlung Zangbo River is the largest river on the Tibetan Plateau. The vegetation in the Yarlung Zangbo River Basin (YZRB) has a significant influence on the biological processes of the Tibetan Plateau [27,28]. The fragile ecological environment, especially the state of vegetation in the YZRB, is sensitive to temperature and precipitation changes [29]. Owing to the high elevation and complex topography, there is a lack of hydro-meteorological gauges and hence a lack of data in the YZRB, which restricts the application of dynamic models and presents challenges for assessing the sensitivity of each vegetation type in the YZRB to climate change. The relationship between vegetation indices and climatic variables has been investigated by previous studies [20,23]. However, statistical modeling of vegetation and quantitative assessment of the sensitivity to climate change for different vegetation types in the YZRB are relatively rare. It is difficult to apply regression equation models in the YZRB owing to the multiple climate zones, complex topography, and diversity of vegetation. However, machine learning may be able to overcome these problems. Ensemble learning methods, such as random forest (RF), can not only simulate the relationship between vegetation indices and climatic variables but also identify climatic variables' contribution to vegetation growth, which helps in the understanding of the climatic variables' time-lag effects.

The objectives of this paper are to: (i) construct statistical vegetation models using machine learning methods, (ii) quantitatively assess the sensitivity of each vegetation type in the YZRB to climate change, and (iii) explore the time-lag effects for each vegetation type through correlation with the proposed models.

## 2. Materials and Methods

### 2.1. Study Area and Data

#### 2.1.1. Study Area

The Yarlung Zangbo River is one of the highest rivers in the world, with a length of 2229 km and a drainage area of  $2.42 \times 10^5$  km<sup>2</sup>. The YZRB is long and narrow, running from west to east, with the Himalayas to the south and the Gangdise Mountains to the north [27,30]. The topography of the YZRB changes from mountains to plains and there are both perennial snow-covered areas with an altitude of more than 7000 masl and hot and humid valleys with an altitude of less than 200 masl (Figure 1a).

The climate varies across the basin. The upper reaches have a plateau cold temperate climate, while the middle reaches have a plateau temperate climate, and the lower reaches have a tropical and subtropical climate. The temperature increases from northwest to southeast, and precipitation increases from the upper to lower reaches [29]. Because of these climatic differences, the vegetation in the YZRB shows clear spatial heterogeneity [31]. There is mainly Alpine Vegetation (17.6%), Meadow (35.5%), and Scrub (13.3%) in the upper and middle reaches, while Meadow and Steppe (17.1%) are distributed across the basin. The main vegetation in the lower reaches is Cultivated Vegetation (1.8%), Broadleaf Forest

(5.3%), and Needleleaf Forest (5.9%) (Figure 1b). In this paper, the YZRB was divided into 32 sub-catchments based on the hydro-climatic characteristics and watershed boundaries (Figure 1c).

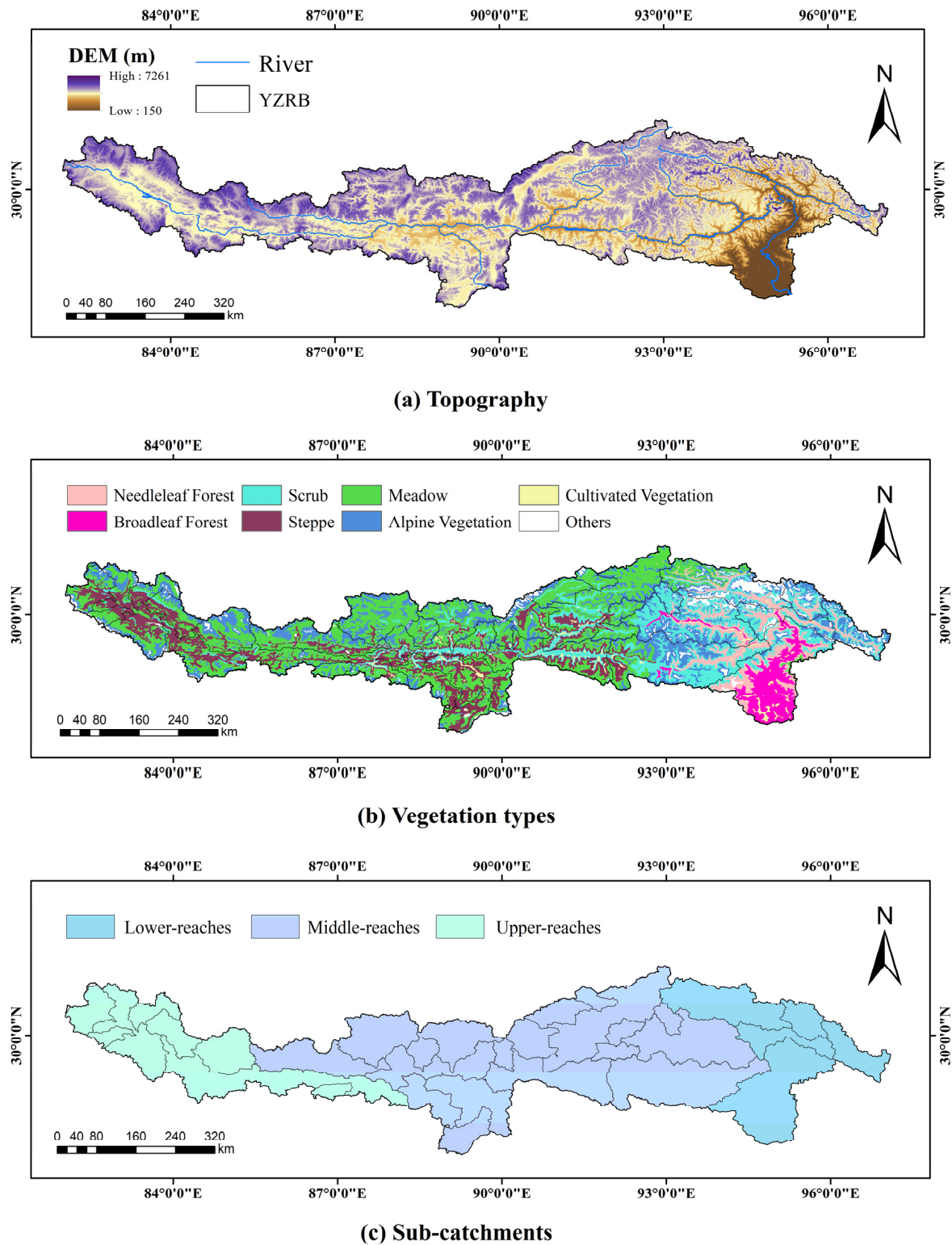


**Figure 1.** The topography, vegetation types, and sub-catchments of the Yarlung Zangbo River Basin (YZRB) ((a) Topography, (b) Vegetation types, (c) Sub-catchments).

### 2.1.2. Data Collection

The China Meteorological Forcing Dataset (CMFD) used in this paper was generated from the Institute of Tibetan Plateau Research of the Chinese Academy of Sciences (<http://westdc.westgis.ac.cn/>, accessed on 10 May 2021). The CMFD's spatial and temporal resolutions are 0.1° and 3 h. We calculated monthly temperature and precipitation for each pixel by averaging the 3-hourly temperature values and summing the 3-hourly precipitation values over each month. Furthermore, the monthly temperature and precipitation of each vegetation type were calculated by averaging the values of pixels of the corresponding vegetation.

The Global Inventory Monitoring and Modeling System NDVI dataset used in this study was generated from NOAA's advanced high-resolution radiometer (<https://ecocast.arc.nasa.gov/data/pub/gimms/>, accessed on 10 May 2021), with a spatial resolution of 8 km. The monthly NDVI data of each vegetation was also calculated by averaging NDVI values of pixels of the corresponding vegetation.

## 2.2. Methodology

### 2.2.1. NDVI Models

Three machine learning models, including multiple linear regression (MLR), support vector machine (SVM), and RF, were used to simulate NDVI changes. All the models were implemented in Python 3.7 using the scikit-learn package version 0.21.3.

MLR relies on a matrix of regression coefficients and is often used to simulate the dependent variable values using multiple predictors [32]. It relies on a matrix of regression coefficients which represent the correlations between the dependent and independent variables. SVM represents a supervised machine learning method based on statistical learning. Support vector regression is an extension of the support vector machine method and can express the non-linear relationship between the dependent variable and independent variables. Therefore, generalized regression efficiency is achieved based on the minimization of training errors [33].

RF was first proposed by Breiman in 2001 as a new machine learning model based on classification and regression tree (CART) algorithms [34]. RF estimates the error of the model through the out-of-bag error (EOOB) with built-in cross-validation running in parallel to the training process. This model can evaluate variable importance by randomly permuting these variables and observing the difference in model performance using OOB samples. At the end of the process, RF obtains variable importance by averaging the differences, which are then normalized by the standard deviation. This method is widely used by hydrologists in classification and regression analysis [25], statistical downscaling [35], and hydrological modeling [26].

The monthly NDVI for different vegetation types were modeled using 12 different climatic variables including temperature and precipitation at time lags of 0–5 months (Table 1). Then, we used data from the first 70% of years for model calibration and the remaining 30% for validation. Finally, Nash–Sutcliffe coefficient (NASH), root mean square errors (RMSE), mean absolute percentage error (MAE), correlation coefficient ( $r$ ), and normalized mean bias (NMB) were used to assess the predictive performance of the models [26,36,37], which were defined as:

$$\text{NASH} = 1 - \frac{\sum_{i=1}^n (Y_{i,obs} - Y_{i,sim})^2}{\sum_{i=1}^n (Y_{i,obs} - \bar{Y}_{obs})^2} \quad (1)$$

$$\text{RMSE} = \sqrt{\frac{\sum_{i=1}^n (Y_{i,obs} - Y_{i,sim})^2}{n}} \quad (2)$$

$$\text{MAE} = \frac{\sum_{i=1}^n |Y_{i,obs} - Y_{i,sim}|}{n} \quad (3)$$

$$r = \frac{\sum_{i=1}^n [(Y_{i,obs} - \overline{Y_{obs}})(Y_{i,sim} - \overline{Y_{sim}})]}{\sqrt{\sum_{i=1}^n (Y_{i,obs} - \overline{Y_{obs}})^2} \sqrt{\sum_{i=1}^n (Y_{i,sim} - \overline{Y_{sim}})^2}} \quad (4)$$

$$\text{NMB (\%)} = \frac{\sum_{i=1}^n (Y_{i,sim} - Y_{i,obs})}{\sum_{i=1}^n (Y_{i,obs})} * 100 \quad (5)$$

where  $Y_{i,obs}$  represents the vector of the observed predictands of number  $i$ ,  $Y_{i,sim}$  is the vector of the simulated predictands of number  $i$ ,  $\overline{Y_{obs}}$  is the mean of the observed predictands, and  $\overline{Y_{sim}}$  is the mean of the simulated predictands.

**Table 1.** The climatic variables for model input.

Climatic Variables	Temperature					Precipitation						
Time lags (month)	0	1	2	3	4	5	0	1	2	3	4	5
Input factors	t0	t1	t2	t3	t4	t5	p0	p1	p2	p3	p4	p5

### 2.2.2. The Sensitivity of NDVI to Climate Change

The sensitivity to temperature and precipitation changes for different vegetation types were assessed by simulated NDVI changes using hypothetical climatic scenarios and observed climate data. According to previous studies on climate prediction of the Tibetan Plateau, the temperature was expected to change by 0.9–2.3 °C, while the precipitation was expected to change by −3–16% in the middle of this century [38–40]. We used eight climatic scenarios to assess the sensitivity, which was defined as: (i) −2.0 °C to 2.0 °C temperature change in 0.5 °C intervals; and (ii) −20% to 20% precipitation change in 5% intervals. In this paper, the sensitivity is defined as:

$$\varepsilon = \frac{NDVI_h - NDVI_o}{NDVI_o} \quad (6)$$

where  $\varepsilon$  is the sensitivity to climate change;  $NDVI_o$  is the simulated NDVI using observed data;  $NDVI_h$  is the simulated NDVI using hypothetical climatic scenarios.

## 3. Results

### 3.1. The Spatiotemporal Variations of the NDVI and Climatic Variables

The inter-annual variations in the NDVI and climatic variables from 1982 to 2015 were shown in Figure 2. According to Figure 2a,b, the precipitation increased insignificantly at the rate of 19 mm/10a ( $R^2 = 0.11$ ,  $p = 0.031$ ), while temperature increased significantly at the rate of 0.42 °C/10a ( $R^2 = 0.56$ ,  $p = 0.000$ ). The NDVI did not show a significant trend ( $R^2 = 0.18$ ,  $p = 0.007$ ). This finding is in accordance with previous studies that non-significant increasing trends in precipitation and NDVI were observed in the YZRB (with low  $R^2$  value for precipitation and NDVI) [23,27]. According to Figure 2c,d, although the NDVI of the YZRB showed a slightly increasing trend, the NDVI trend of different vegetation types showed clear variations. The trends of different vegetation types were detected by summarizing the slopes of all pixels for each vegetation type with a violin plot (Figure 2d). It was shown that Needleleaf Forest, Scrub, and Alpine Vegetation had a greening trend in most areas (slope > 0), although there was also a declining trend in some areas (slope < 0). Steppe and Meadow did not show a clear trend. Broadleaf Forest, which was distributed in the lower reaches, mainly showed a declining trend.

The spatial distribution of the multi-annual mean values of temperature, precipitation, and the NDVI across the YZRB as well as their trends was detected by the Mann–Kendall trend test and Sen’s slope [7,41] (Figure 3). From Figure 3a–c, we can observe that temperature, precipitation, and the NDVI of the YZRB increased gradually from the upper to the lower reaches. As Figure 3d–f shows, most of the temperature pixels exhibited significant increasing trends, and temperature in the upper reaches increased faster than that in other regions. However, the precipitation and the NDVI trends showed high spatial variability.

For precipitation, the eastern part of the upper reaches and the northern part of the lower reaches exhibited significant decreasing trends while the other regions showed significant increasing trends. This finding is in accordance with previous studies that some areas in the upper and lower reaches showed a decreasing trend [20]. For the NDVI, most pixels in the upper and middle reaches exhibited significant increasing trends, while parts of the lower reaches and a minority of parts of the upper reaches showed significant decreasing trends.

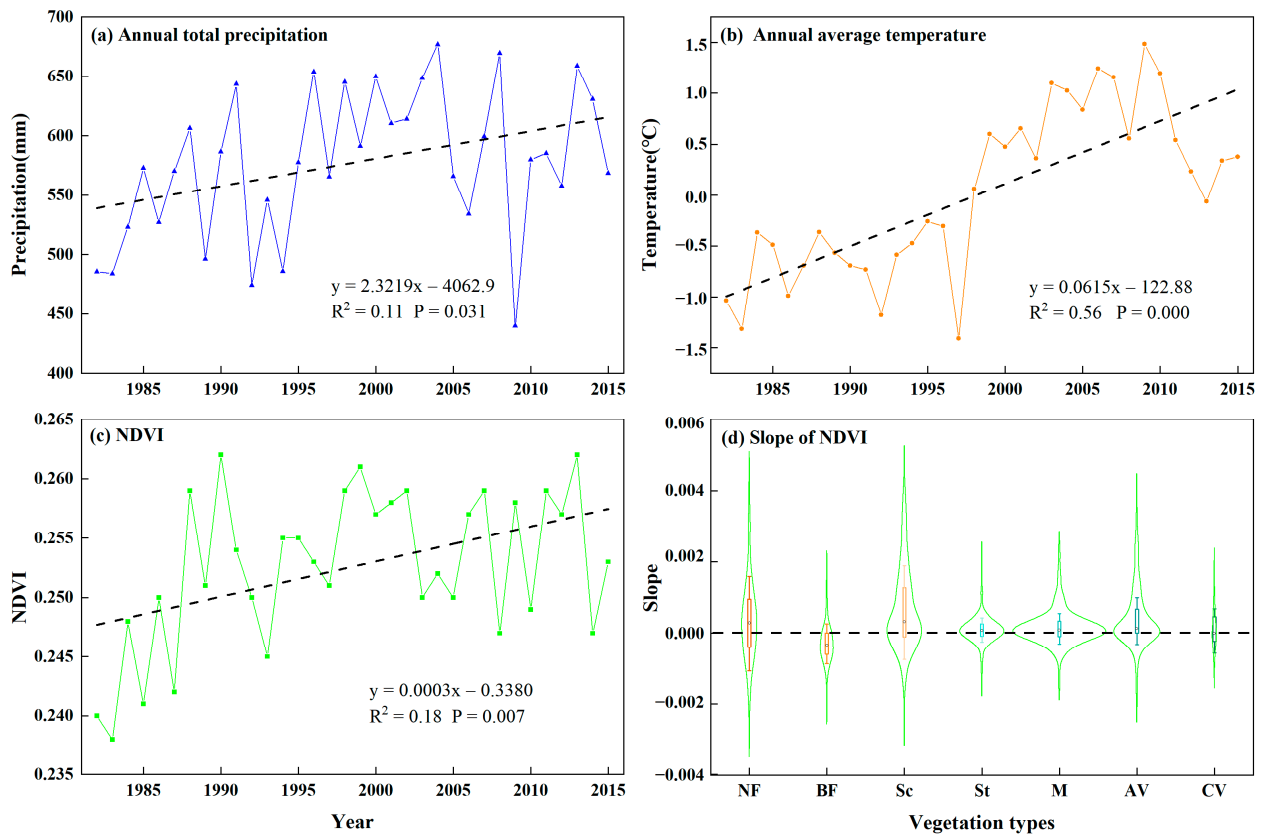


**Figure 2.** Basin-averaged inter-annual variations in the Normalized Difference Vegetation Index (NDVI) and climatic variables as well as the slope of the NDVI for each vegetation type in the YZRB ((a) Annual total precipitation, (b) Annual average temperature, (c) NDVI, (d) Slope of NDVI) (NF: Needleleaf Forest, BF: Broadleaf Forest, Sc: Scrub, St: Steppe, M: Meadow, AV: Alpine Vegetation, CV: Cultivated Vegetation).

### 3.2. NDVI Modeling

The results for the three machine learning models—MLR, SVM, and RF—that were selected to simulate the relationships between vegetation and climatic variables are summarized in Table 2.

According to the five metrics shown in Table 2, RF models were better than the comparative models and performed well in the calibration and validation period. The average NASH of the MLR, SVM, and RF was 0.83, 0.75, and 0.98 in the calibration period and 0.81, 0.78, and 0.84 in the validation period. The observed and predicted monthly NDVI series in the validation period from the random forest for different vegetation types were shown in Figure 4. They illustrated the good performance of NDVI modeling using RF for all vegetation types.

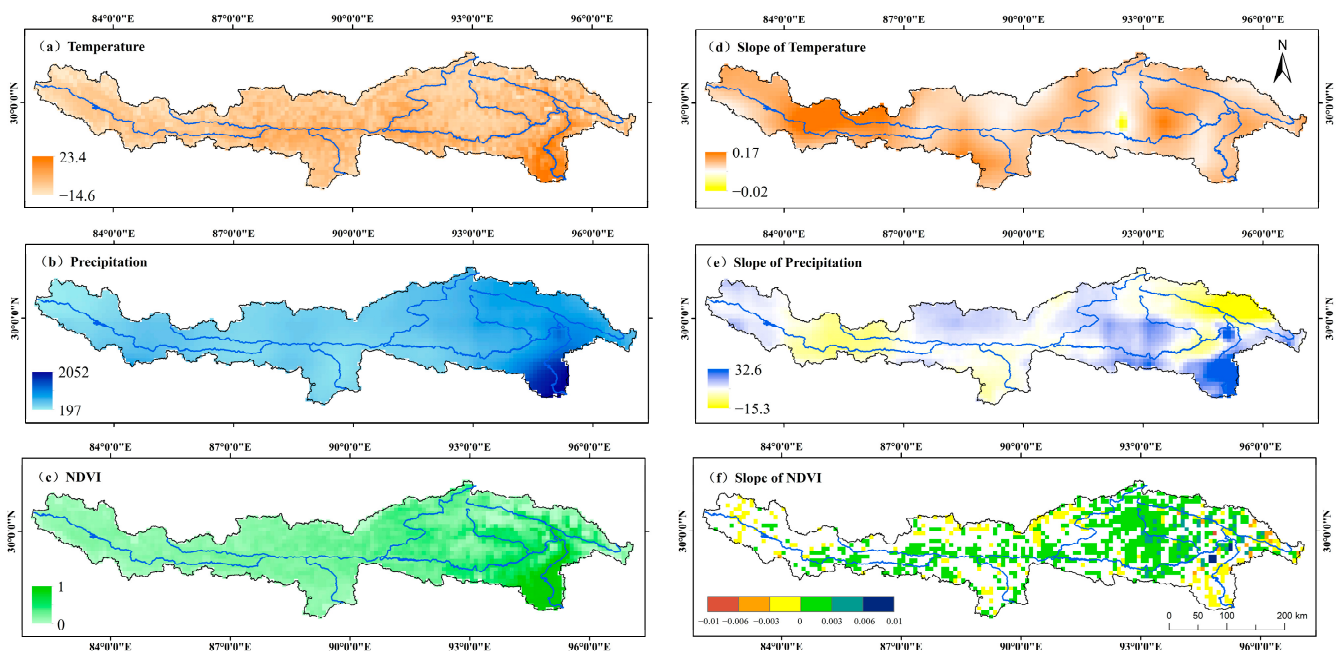


**Figure 3.** Basin-averaged inter-annual variations of climatic variables and the NDVI as well as their slope in the YZRB ((a) Temperature, (b) Precipitation, (c) NDVI, (d) Slope of temperature, (e) Slope of precipitation, (f) Slope of NDVI).

**Table 2.** Performance evaluation of all models in the calibration and validation period.

Vegetation Types	Models	Calibration					Validation				
		NASH	RMSE	MAE	r	NMB	NASH	RMSE	MAE	r	NMB
Needleleaf Forest	MLR	0.67	0.04	0.03	0.82	0.00	0.64	0.05	0.04	0.80	−0.28
	SVM	0.65	0.04	0.04	0.81	0.23	0.59	0.04	0.03	0.72	−1.53
	RF	0.95	0.02	0.01	0.98	0.04	0.61	0.05	0.04	0.78	−0.85
Broadleaf Forest	MLR	0.68	0.03	0.03	0.82	0.00	0.68	0.03	0.03	0.83	0.46
	SVM	0.81	0.04	0.03	0.91	1.69	0.62	0.05	0.04	0.78	−3.52
	RF	0.95	0.01	0.01	0.98	−0.01	0.65	0.04	0.04	0.81	−0.01
Scrub	MLR	0.86	0.04	0.03	0.93	0.00	0.82	0.04	0.03	0.91	−2.11
	SVM	0.81	0.04	0.03	0.91	0.16	0.80	0.04	0.03	0.89	−1.00
	RF	0.99	0.01	0.01	0.99	0.01	0.87	0.03	0.03	0.94	−3.75
Steppe	MLR	0.94	0.02	0.01	0.97	0.00	0.92	0.02	0.02	0.96	1.03
	SVM	0.71	0.03	0.03	0.85	3.07	0.89	0.02	0.02	0.95	2.11
	RF	1.00	0.00	0.00	1.00	−0.06	0.96	0.01	0.01	0.98	−0.71
Meadow	MLR	0.94	0.02	0.02	0.97	0.00	0.94	0.02	0.02	0.97	0.48
	SVM	0.67	0.03	0.03	0.81	6.73	0.93	0.02	0.02	0.98	0.55
	RF	1.00	0.01	0.00	1.00	0.02	0.97	0.01	0.01	0.99	−0.93
Alpine Vegetation	MLR	0.91	0.02	0.02	0.96	0.00	0.89	0.02	0.02	0.95	−3.58
	SVM	0.68	0.03	0.03	0.83	6.77	0.87	0.03	0.03	0.94	7.11
	RF	0.99	0.01	0.00	1.00	0.02	0.94	0.02	0.01	0.97	−4.52
Cultivated Vegetation	MLR	0.83	0.03	0.02	0.91	0.00	0.79	0.03	0.02	0.89	−1.08
	SVM	0.92	0.02	0.02	0.96	0.19	0.76	0.04	0.03	0.87	3.11
	RF	0.99	0.01	0.01	0.99	0.04	0.87	0.03	0.02	0.93	−2.38
Average	MLR	0.83	0.03	0.02	0.91	0.00	0.81	0.03	0.02	0.90	−0.73
	SVM	0.75	0.03	0.03	0.87	1.73	0.78	0.04	0.03	0.88	0.76
	RF	0.98	0.01	0.01	0.99	0.00	0.84	0.03	0.02	0.91	−2.26

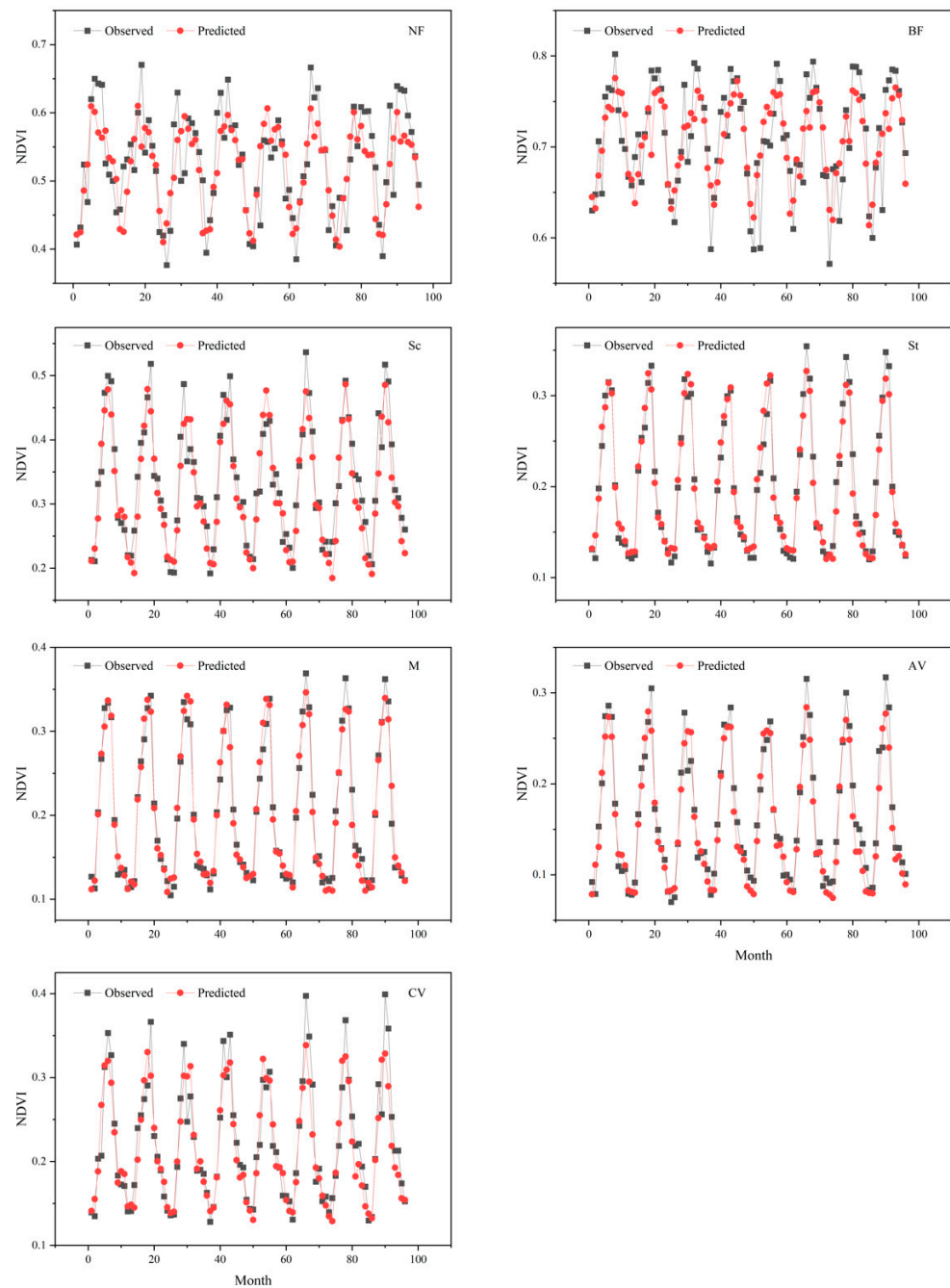
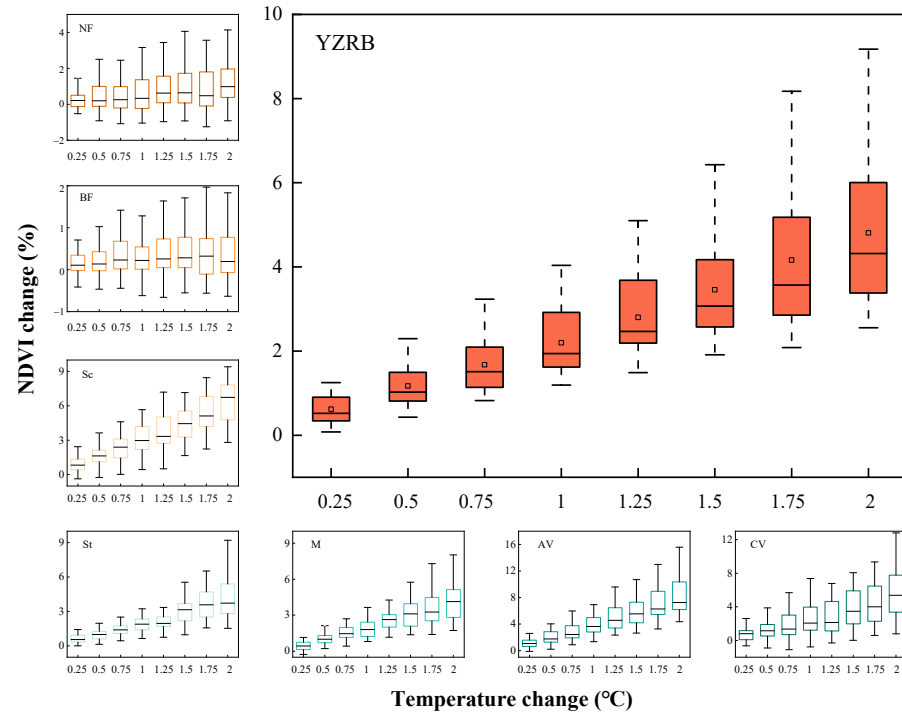


**Figure 4.** The observed and predicted NDVI series in the validation period from the random forest for different vegetation types.

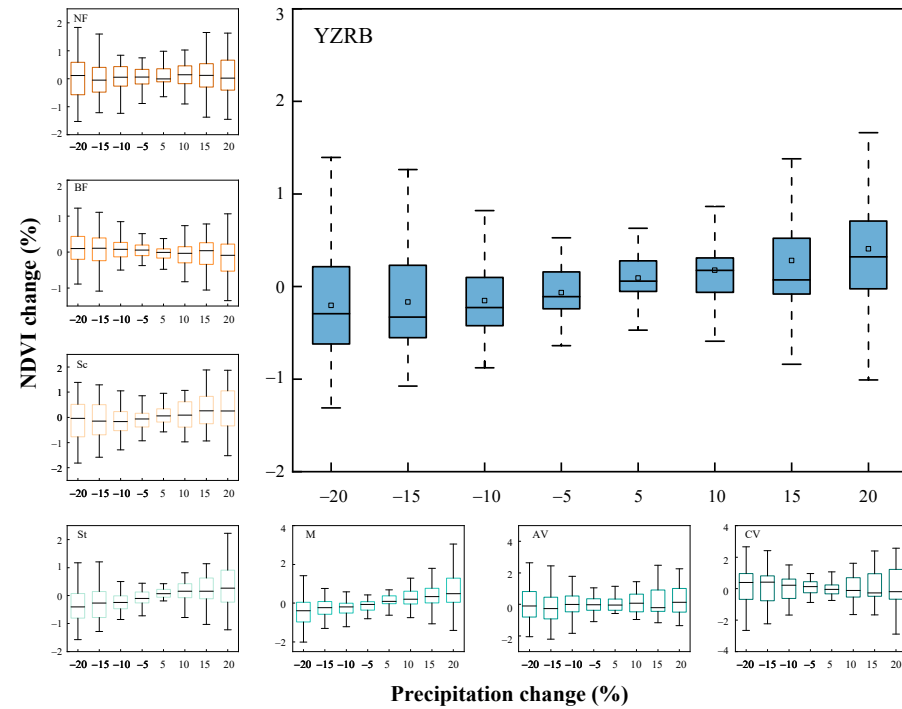
### 3.3. The Sensitivity to Climate Change for Different Vegetation Types

The sensitivity to temperature and precipitation changes for different vegetation types was assessed based on RF models that showed the best performance, which was shown in Figures 5 and 6. The results indicated that the NDVI of each vegetation type would rise with an increase in temperature. In general, the NDVI of the YZRB increased by 1.60–4.68%, when the temperature increased by 1.5 °C. The sensitivity of different vegetation types to temperature differed (Figure 5a). We found that the vegetation located in the upper and middle reaches, including Alpine Vegetation, Meadow, Steppe, Scrub, and Cultivated Vegetation, was sensitive to temperature. However, the vegetation in the lower reaches, such as Needleleaf Forest and Broadleaf Forest, was not sensitive to temperature changes. Spatially, the vegetation was more sensitive to temperature in the upper and middle reaches;

in other words, in higher altitude areas with lower temperatures, the vegetation was more sensitive to temperature changes (Figure 6a). These findings are consistent with the results of similar studies. Park et al. [42] found vegetation was more sensitive to temperature changes in a cold environment. Sun et al. [23] pointed out that higher temperatures would produce more snow-melt water for vegetation to use, which was important in the cold and dry regions of the YZRB.



(a) The response of NDVI to temperature



(b) The response of NDVI to precipitation

Figure 5. The response to temperature and precipitation for different vegetation types on an annual scale (a) The response of NDVI to temperature, (b) The response of NDVI to Precipitation).

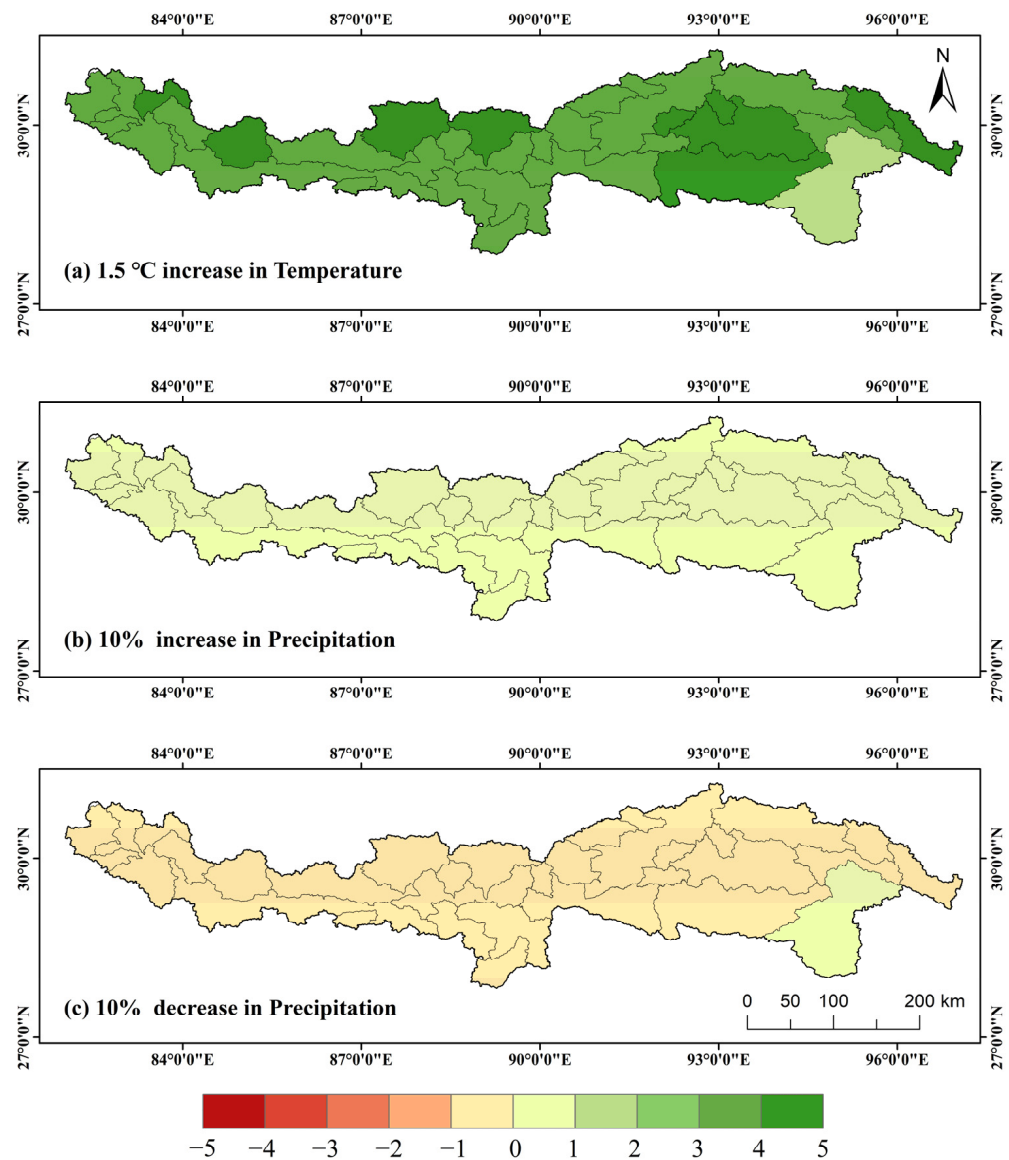


**Figure 6.** The distribution of the response to temperature and precipitation changes on an annual scale in the YZRB ((a) 1.5 °C increase in temperature, (b) 10% increase in precipitation, (c) 10% decrease in precipitation).

We found that the vegetation was more sensitive to temperature than to precipitation in the YZRB, which concurs with previous studies [43,44]. Although the results indicated slightly positive responses of the vegetation to precipitation generally, i.e., the NDVI increased with an increase in precipitation, the response of different vegetation types to precipitation exhibited a wide variation (Figure 5b). Meadow, Steppe, and Scrub, which were mainly located in the arid and semi-arid regions, were slightly sensitive to precipitation. However, the other vegetation types, including Alpine Vegetation, Cultivated Vegetation, Needleleaf Forest, and Broadleaf Forest, were not sensitive to precipitation. According to Figure 6b,c, the NDVI of the YZRB would increase by 0.06–0.24% when the precipitation increased by 10%. The NDVI showed a slightly positive response (<1%) to precipitation in the scenarios with a precipitation increase of 10% or a decrease of 10% in most sub-catchments. However, the NDVI showed only a slight increase in both scenarios in the lower reaches because of the non-sensitive response of the vegetation in the catchment, which was dominated by Needleleaf Forest and Broadleaf Forest.

The sensitivity to temperature and precipitation changes on a monthly scale was also investigated according to the outputs of the NDVI models in three hypothetical climate

scenarios, i.e., 1.5 °C increase in temperature, 10% increase in precipitation, and 10% decrease in precipitation. As shown in Figure 7, the monthly NDVI was more sensitive to temperature than to precipitation. In Figure 7a, the monthly distributions of the sensitivity to climate change were similar for the seven vegetation types, with a peak in April to June and a trough in August to October. All vegetation types were more sensitive to temperature increases at the start of spring and summer. The reason may be that the vegetation is supplied with sufficient snow-melt water as the temperature rises in the period [45,46]. However, we also found that Needleleaf Forest and Broadleaf Forest had a slightly negative response to temperature in autumn, which may result from the increasing evaporation when temperatures are higher [47,48]. For precipitation (Figure 7b,c), the difference in the monthly distribution of the sensitivity to precipitation was not obvious, which indicated that precipitation was not the main factor affecting vegetation growth in the YZRB.

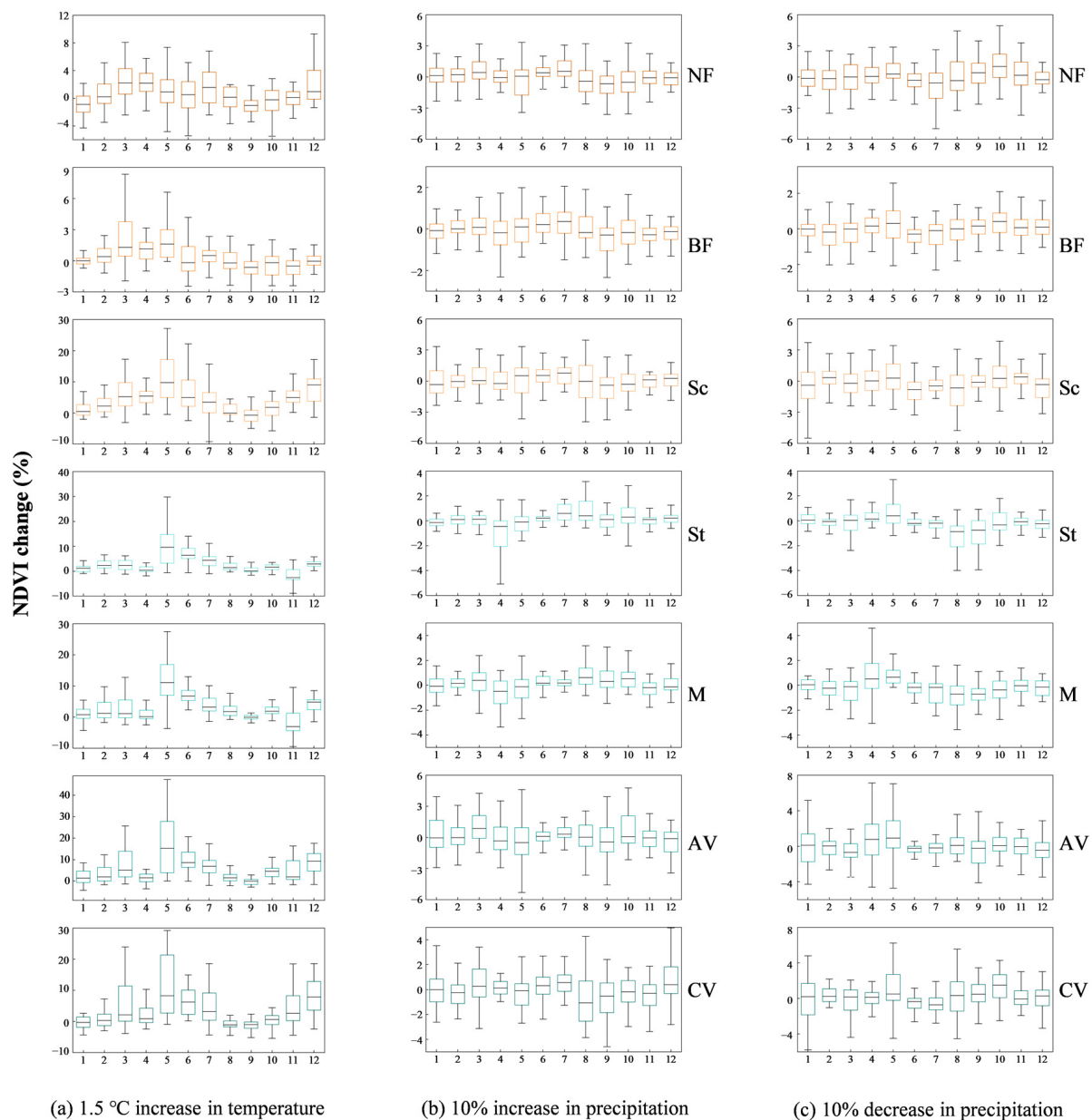


**Figure 7.** The response to temperature and precipitation for different vegetation types on a monthly scale ((a) 1.5 °C increase in temperature, (b) 10% increase in precipitation, (c) 10% decrease in precipitation).

We also identified the seasonal distribution of the sensitivity to temperature changes (Figure 8), which were the average sensitivities for different seasonal months. The NDVI is most sensitive to a temperature change in spring, which is predicted to rise by approximately 3.4–7.8%. Spatially, the NDVI appears less sensitive in the south of the lower reaches, which is in accordance with the spatial distribution of response on an annual scale. Because the monthly NDVI is not sensitive to precipitation and shows a positive sensitivity of <1% to precipitation change, its seasonal distributions are not included in this paper.

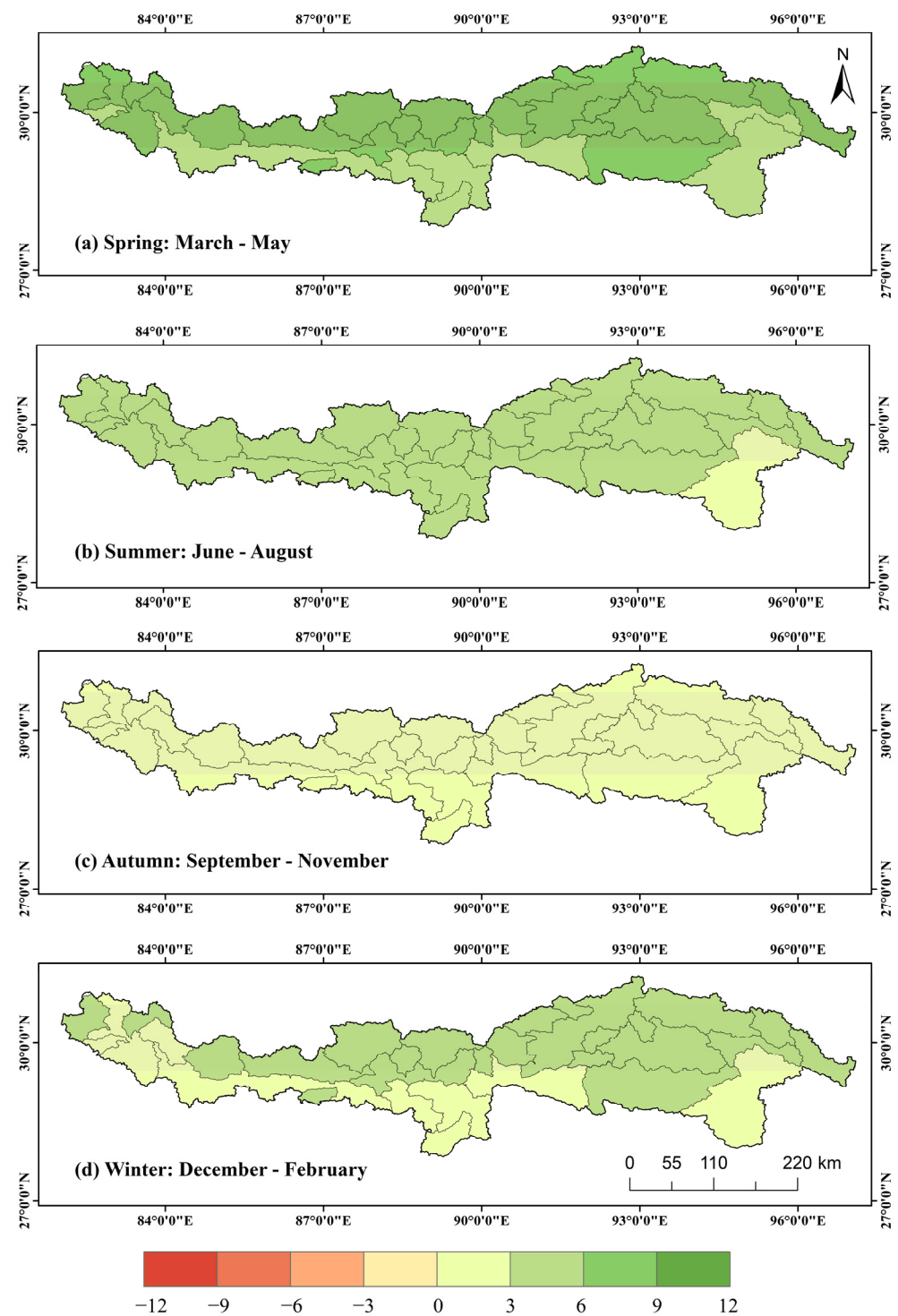


**Figure 8.** The distribution of the responses to a temperature increase (1.5 °C) on a monthly scale in the YZRB ((a) Spring, (b) Summer, (c) Autumn, (d) Winter).

## 4. Discussion

### 4.1. The Time-Lag Effects of Temperature and Precipitation on Different Types of Vegetation

The time-lag effects of temperature and precipitation on different types of vegetation were investigated through their correlation coefficients at time lags of 0–3 months (Table 3). We found that the highest correlations for Scrub, Steppe, Meadow, Alpine Vegetation, and Cultivated Vegetation in response to temperature and precipitation were with a 1-month lag. However, the highest correlations for Needleleaf Forest and Broadleaf Forest were with 2-month lag and 3-month lag for temperature, respectively, and with a 3-month lag for both for precipitation. We found that the most correlated variables for all vegetation types were all temperatures with different time lags. The correlation coefficients varied from 0.75 to 0.89.

**Table 3.** The correlation coefficients between the NDVI of different vegetation types and temperature and precipitation at time lags of 0–3 months.

The NDVI of Different Vegetation Types	Input Factors							
	t0	p0	t1	p1	t2	p2	t3	p3
Needleleaf Forest	0.32	0.09	0.61	0.44	<b>0.76</b>	0.65	0.72	<b>0.67</b>
Broadleaf Forest	0.02	0.34	0.34	0.11	0.63	0.42	<b>0.75</b>	<b>0.58</b>
Scrub	0.71	0.65	<b>0.86</b>	<b>0.80</b>	0.81	0.70	0.57	0.44
Steppe	0.84	0.81	<b>0.89</b>	<b>0.84</b>	0.73	0.53	0.39	0.11
Meadow	0.85	0.84	<b>0.88</b>	<b>0.85</b>	0.72	0.52	0.37	0.09
Alpine Vegetation	0.80	0.77	<b>0.89</b>	<b>0.85</b>	0.77	0.63	0.47	0.28
Cultivated Vegetation	0.73	0.66	<b>0.85</b>	<b>0.81</b>	0.77	0.70	0.51	0.42

The RF model was able to successfully evaluate the contributions of the predictors based on its built-in variable importance evaluation processes. We plotted both the rank of the correlation coefficients (Figure 9a) and the rank of the predictors' importance (Figure 9b) to explore the time-lag effects of climatic variables on each type of vegetation. The results of the two methods were similar, although some differences remained. Both methods indicated the NDVI was more sensitive to temperature than to precipitation for all vegetation types. In the two methods, the NDVI of Needleleaf Forest, Broadleaf Forest, Scrub, and Cultivated Vegetation had the same time lag to temperature, while the NDVI of Steppe, Meadow, and Alpine Vegetation had a 1-month lag to temperature in the correlation analysis and a 0-month lag in the RF importance evaluation. However, we found that 0-month was the second most correlated period for temperature in the correlation analysis and 1-month was the second important period in the RF importance evaluation. The time lags of temperature for different vegetation types were very similar for the two methods.

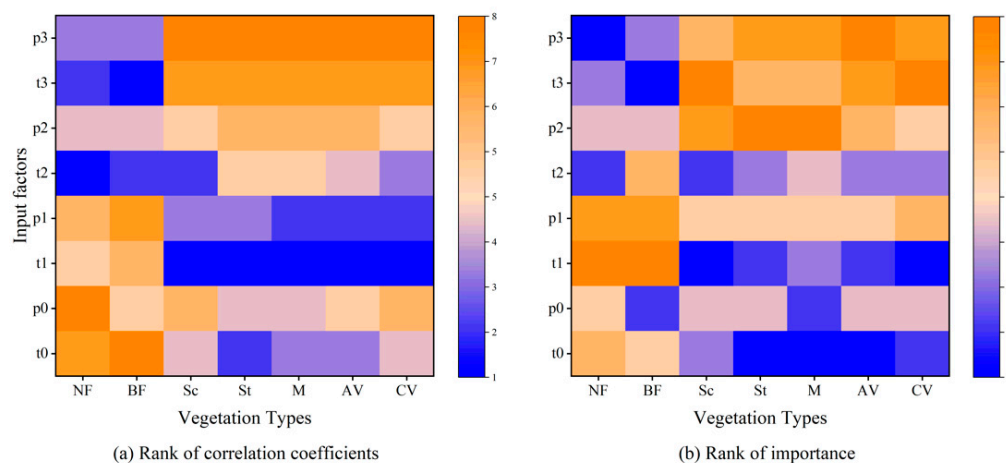


**Figure 9.** The correlations between the NDVI and climatic variables at time lags of 0–3 months for different vegetation types ((a) Rank of correlation coefficients, (b) Rank of importance).

The time lags for precipitation in the different vegetation types showed higher variation. Although the time lags for Needleleaf Forest were all 3 months, those of Scrub, Steppe, Meadow, Alpine Vegetation, and Cultivated Vegetation were all 0–1 month for the two methods. The reason for the differences may be that the RF importance evaluation considered the inherent correlation of the climate variables and showed more differences between less important variables than that of the correlation analysis [49,50].

#### 4.2. Limitations

There were some limitations in our research. One limitation was that vegetation change or evolution in the YZRB was not considered in this study, which may lead to inaccuracies in the simulation. At the same time, we explored the effects of temperature and precipitation disturbances on vegetation separately but did not consider the combined effects. Vegetation is also affected by variables, such as human activities, soil moisture content, and CO<sub>2</sub> [51,52]. We will explore these factors as part of the model inputs in our future research. In addition, this study established basin-scale machine learning models based on different vegetation types. In the future, we will try to explore the relationship between NDVI and climatic variables at higher resolutions. Vegetation cover is deeply affected by global climate change and its sensitivity to climatic variables has attracted worldwide attention. Due to the differences in ecological patterns and climatic conditions, the sensitivity of vegetation cover to climate change varies significantly [53,54]. This is the first attempt to assess the vegetation sensitivity of YZRB to climate change, which is one of the highest basins of the world with a complex topography and diverse vegetation. Our conclusions will not only support the land planning and water resources management of the Tibetan Plateau but also have reference value for vegetation sensitivities studies of high-altitude basins [55–57].

#### 5. Conclusions

We assessed the sensitivity to climate change for different vegetation types in the YZRB using machine learning methods. To analyze spatiotemporal variability, three machine learning models, MLR, SVM, and RF, were adopted to simulate the relationships between vegetation and climatic variables. RF, the best performing model, was then used to quantitatively evaluate the sensitivity of each vegetation type to temperature and precipitation change. The time-lag effects of each vegetation type on climate were also analyzed with the proposed models. The main findings of this study are summarized as follows.

(1) RF models successfully simulated the relationships between the NDVI and climatic variables, which were better than MLR models and SVM models. The average NASH of MLR, SVM, and RF was 0.83, 0.75, and 0.98 in the calibration period and 0.81, 0.78, and 0.84 in the validation period. RF models exhibited the highest simulation efficiency according to the four metrics.

(2) Different vegetation types responded positively to temperature and precipitation changes on an annual scale, but the vegetation was more sensitive to temperature than to precipitation in the YZRB. The NDVI was predicted to increase by 1.60–4.68% when the temperature increased by 1.5 °C, while it only changed by 0.06–0.24% when the precipitation increased by 10% in the YZRB. The NDVI was more sensitive to temperature changes in spring and summer on a monthly scale. The NDVI was also more sensitive to temperature rises in the upper and middle reaches, where the existing temperature was cooler.

(3) The time-lag effects of climate for each vegetation were analyzed using correlation analysis and RF importance evaluation. For temperature, Needleleaf Forest and Broadleaf Forest showed a 2-month lag and 3-month lag, respectively; Scrub and Cultivated Vegetation both showed a 1-month lag, while Steppe, Meadow, and Alpine Vegetation showed a 0–1 month lag. For precipitation, Needleleaf Forest and Broadleaf Forest also had longer time lags than those of other vegetation types, although the two methods had slightly different results.

**Author Contributions:** Conceptualization, L.C. and B.P.; data curation, L.C., B.P., C.B. and M.R.; formal analysis, L.C.; software, L.C. and G.Z.; validation, G.Z., C.B. and M.R.; writing—original draft preparation, L.C.; writing—review and editing, B.P., D.P., D.Z. and Z.Z. All authors have read and agreed to the published version of the manuscript.

**Funding:** This research was funded by The National Natural Science Foundation of China (51879008 and 52179003).

**Institutional Review Board Statement:** Not applicable.

**Informed Consent Statement:** Not applicable.

**Data Availability Statement:** Not applicable.

**Acknowledgments:** We thank Leonie Seabrook, PhD and Liwen Bianji (Edanz) ([www.liwenbianji.cn](http://www.liwenbianji.cn), accessed on 15 January 2022) for editing the language of a draft of this manuscript.

**Conflicts of Interest:** The authors declare no conflict of interest.

## References

- Piao, S.; Mohammat, A.; Fang, J.; Cai, Q.; Feng, J. NDVI-based increase in growth of temperate grasslands and its responses to climate changes in China. *Glob. Environ. Chang.* **2006**, *16*, 340–348. [[CrossRef](#)]
- Huang, S.; Ming, B.; Huang, Q.; Leng, G.; Hou, B. A case study on a combination NDVI forecasting model based on the entropy weight method. *Water Resour. Manag.* **2017**, *31*, 3667–3681. [[CrossRef](#)]
- Kumar, A.; Kumar, M.; Pandey, R.; Yu, Z.G.; Cabral-Pinto, M. Forest soil nutrient stocks along altitudinal range of Uttarakhand Himalayas: An aid to Nature Based Climate Solutions. *Catena* **2021**, *207*, 105667. [[CrossRef](#)]
- Lemordant, L.; Gentine, P.; Swann, A.S.; Cook, B.I.; Scheff, J. Critical impact of vegetation physiology on the continental hydrologic cycle in response to increasing CO<sub>2</sub>. *Proc. Natl. Acad. Sci. USA* **2018**, *115*, 4093–4098. [[CrossRef](#)] [[PubMed](#)]
- Wu, D.H.; Zhao, X.; Liang, S.L.; Zhou, T.; Huang, K.C.; Tang, B.J.; Zhao, W.Q. Time-lag effects of global vegetation responses to climate change. *Glob. Chang. Biol.* **2015**, *21*, 3520–3531. [[CrossRef](#)] [[PubMed](#)]
- Seddon, A.W.R.; Macias-Fauria, M.; Long, P.R.; Benz, D.; Willis, K.J. Sensitivity of global terrestrial ecosystems to climate variability. *Nature* **2016**, *531*, 229–232. [[CrossRef](#)]
- Wei, X.; Wang, N.; Luo, P.; Yang, J.; Zhang, J.; Lin, K. Spatiotemporal assessment of land marketization and its driving forces for sustainable Urban–Rural development in Shaanxi Province in China. *Sustainability* **2021**, *13*, 7755. [[CrossRef](#)]
- Luo, P.; Mu, Y.; Wang, S.; Zhu, W.; Mishra, B.K.; Huo, A.; Zhou, M.; Lyu, J.; Hu, M.; Duan, W.; et al. Exploring sustainable solutions for the water environment in Chinese and Southeast Asian cities. *Ambio* **2021**, *51*, 1199–1218. [[CrossRef](#)] [[PubMed](#)]
- Fu, J.; Niu, J.; Sivakumar, B. Prediction of vegetation anomalies over an inland river basin in north-western China. *Hydrol. Process.* **2018**, *32*, 1814–1827. [[CrossRef](#)]
- Ge, J.; Meng, B.; Liang, T.; Feng, Q.; Gao, J.; Yang, S.; Huang, X.; Xie, H. Modeling alpine grassland cover based on MODIS data and support vector machine regression in the headwater region of the Huanghe River, China. *Remote Sens. Environ.* **2018**, *218*, 162–173. [[CrossRef](#)]
- Kim, J.B.; Kerns, B.K.; Drapek, R.J.; Pitts, G.S.; Halofsky, J.E. Simulating vegetation response to climate change in the Blue Mountains with MC2 dynamic global vegetation model. *Clim. Serv.* **2018**, *10*, 20–32. [[CrossRef](#)]
- Bao, Z.; Zhang, J.; Wang, G.; Guan, T.; Jin, J.; Liu, Y.; Li, M.; Ma, T. The sensitivity of vegetation cover to climate change in multiple climatic zones using machine learning algorithms. *Ecol. Indic.* **2021**, *124*, 107443. [[CrossRef](#)]
- Gerten, D.; Schaphoff, S.; Haberlandt, U.; Lucht, W.; Sitch, S. Terrestrial vegetation and water balance—Hydrological evaluation of a dynamic global vegetation model. *J. Hydrol.* **2004**, *286*, 249–270. [[CrossRef](#)]
- Winter, J.M.; Pal, J.S.; Eltahir, E.A.B. Coupling of integrated biosphere simulator to Regional Climate Model Version 3. *J. Clim.* **2009**, *22*, 2743–2757. [[CrossRef](#)]
- Piao, S.; Wang, X.; Ciais, P.; Zhu, B.; Wang, T.A.O.; Liu, J.I.E. Changes in satellite-derived vegetation growth trend in temperate and boreal Eurasia from 1982 to 2006. *Glob. Chang. Biol.* **2011**, *17*, 3228–3239. [[CrossRef](#)]
- Bondeau, A.; Smith, P.C.; Zaehle, S.; Schaphoff, S.; Lucht, W.; Cramer, W.; Gerten, D.; Lotze-Campen, H.; Müller, C.; Reichstein, M.; et al. Modelling the role of agriculture for the 20th century global terrestrial carbon balance. *Glob. Chang. Biol.* **2007**, *13*, 679–706. [[CrossRef](#)]
- Smith, B.; Knorr, W.; Widlowski, J.-L.; Pinty, B.; Gobron, N. Combining remote sensing data with process modeling to monitor boreal conifer forest carbon balances. *For. Ecol. Manag.* **2008**, *255*, 3985–3994. [[CrossRef](#)]
- Schroter, D.; Cramer, W.; Leemans, R.; Prentice, I.C.; Araujo, M.B.; Arnell, N.W.; Bondeau, A.; Bugmann, H.; Carter, T.R.; Gracia, C.A.; et al. Ecosystem service supply and vulnerability to global change in Europe. *Science* **2005**, *310*, 1333–1337. [[CrossRef](#)]
- Zaehle, S.; Sitch, S.; Smith, B.; Hatterman, F. Effects of parameter uncertainties on the modeling of terrestrial biosphere dynamics. *Glob. Biogeochem. Cycles* **2005**, *19*, GB3020. [[CrossRef](#)]

20. Zuo, D.; Han, Y.; Xu, Z.; Li, P.; Ban, C.; Sun, W.; Pang, B.; Peng, D.; Kan, G.; Zhang, R.; et al. Time-lag effects of climatic change and drought on vegetation dynamics in an alpine river basin of the Tibet Plateau, China. *J. Hydrol.* **2021**, *600*, 126532. [[CrossRef](#)]
21. Zheng, K.; Wei, J.Z.; Pei, J.Y.; Cheng, H.; Zhang, X.L.; Huang, F.Q.; Li, F.M.; Ye, J.S. Impacts of climate change and human activities on grassland vegetation variation in the Chinese Loess Plateau. *Sci. Total Environ.* **2019**, *660*, 236–244. [[CrossRef](#)]
22. Yuan, H.H.; Yang, G.J.; Li, C.C.; Wang, Y.J.; Liu, J.G.; Yu, H.Y.; Feng, H.K.; Xu, B.; Zhao, X.Q.; Yang, X.D. Retrieving soybean leaf area index from unmanned aerial vehicle hyperspectral remote sensing: Analysis of RF, ANN, and SVM regression models. *Remote Sens.* **2017**, *9*, 309. [[CrossRef](#)]
23. Sun, W.; Wang, Y.; Fu, Y.H.; Xue, B.; Wang, G.; Yu, J.; Zuo, D.; Xu, Z. Spatial heterogeneity of changes in vegetation growth and their driving forces based on satellite observations of the Yarlung Zangbo River Basin in the Tibetan Plateau. *J. Hydrol.* **2019**, *574*, 324–332. [[CrossRef](#)]
24. Li, H.; Jiang, J.; Chen, B.; Li, Y.; Xu, Y.; Shen, W. Pattern of NDVI-based vegetation greening along an altitudinal gradient in the eastern Himalayas and its response to global warming. *Environ. Monit. Assess.* **2016**, *188*, 186. [[CrossRef](#)]
25. Krakauer, N.; Lakhankar, T.; Anadón, J. Mapping and attributing normalized difference vegetation index trends for Nepal. *Remote Sens.* **2017**, *9*, 986. [[CrossRef](#)]
26. Chi, K.; Pang, B.; Cui, L.; Peng, D.; Zhu, Z.; Zhao, G.; Shi, S. Modelling the vegetation response to climate changes in the Yarlung Zangbo River Basin using random forest. *Water* **2020**, *12*, 1433. [[CrossRef](#)]
27. You, Q.; Kang, S.; Wu, Y.; Yan, Y. Climate change over the Yarlung Zangbo River Basin during 1961–2005. *J. Geogr. Sci.* **2007**, *17*, 409–420. [[CrossRef](#)]
28. Guo, B.; Han, F.; Jiang, L. An improved dimidiated pixel model for vegetation fraction in the Yarlung Zangbo River Basin of Qinghai-Tibet Plateau. *J. Indian Soc. Remote Sens.* **2017**, *46*, 219–231. [[CrossRef](#)]
29. Yang, K.; Ye, B.; Zhou, D.; Wu, B.; Foken, T.; Qin, J.; Zhou, Z. Response of hydrological cycle to recent climate changes in the Tibetan Plateau. *Clim. Chang.* **2011**, *109*, 517–534. [[CrossRef](#)]
30. Li, F.; Xu, Z.; Liu, W.; Zhang, Y. The impact of climate change on runoff in the Yarlung Tsangpo River basin in the Tibetan Plateau. *Stoch. Environ. Res. Risk Assess.* **2013**, *28*, 517–526. [[CrossRef](#)]
31. Xu, Z.X.; Liu, W.; Li, F.P.; Liu, P. Vegetation change and its relationship with precipitation on the southern Tibetan Plateau. *IAHS Publ.* **2013**, *359*, 418–424.
32. Ren, M.; Pang, B.; Xu, Z.; Yue, J.; Zhang, R. Downscaling of daily extreme temperatures in the Yarlung Zangbo River Basin using machine learning techniques. *Theor. Appl. Climatol.* **2018**, *136*, 1275–1288. [[CrossRef](#)]
33. Mohammadi, B.; Mehdizadeh, S. Modeling daily reference evapotranspiration via a novel approach based on support vector regression coupled with whale optimization algorithm. *Agric. Water Manag.* **2020**, *237*, 106145. [[CrossRef](#)]
34. Breiman, L. Random forests. *Mach. Learn.* **2001**, *45*, 5–32. [[CrossRef](#)]
35. Pang, B.; Yue, J.; Zhao, G.; Xu, Z. Statistical Downscaling of Temperature with the Random Forest Model. *Adv. Meteorol.* **2017**, *2017*, 7265178. [[CrossRef](#)]
36. Nash, J.E.; Sutcliffe, J.V. River flow forecasting through conceptual models Part I—A discussion of principles. *J. Hydrol.* **1970**, *3*, 282–290. [[CrossRef](#)]
37. Simon, H.; Baker, K.R.; Phillips, S. Compilation and interpretation of photochemical model performance statistics published between 2006 and 2012. *Atmos. Environ.* **2012**, *61*, 124–139. [[CrossRef](#)]
38. Su, F.G.; Duan, X.L.; Chen, D.L.; Hao, Z.C.; Cuo, L. Evaluation of the global climate, models in the CMIP5 over the Tibetan Plateau. *Int. J. Climatol.* **2013**, *26*, 3187–3208. [[CrossRef](#)]
39. Gao, Q.Z.; Guo, Y.Q.; Xu, H.M.; Ganjurjav, H.; Li, Y.; Wan, Y.F.; Qin, X.B.; Ma, X.; Liu, S. Climate change and its impacts on vegetation distribution and net primary productivity of the alpine ecosystem in the Qinghai-Tibetan Plateau. *Sci. Total Environ.* **2016**, *554*, 34–41. [[CrossRef](#)]
40. Zhang, J.Y.; Lun, Y.R.; Liu, L.; Liu, Y.X.; Li, X.; Xu, Z.X. CMIP6 evaluation and projection of climate change over the Tibetan Plateau. *J. Beijing Norm. Univ. Nat. Sci.* **2022**, *58*, 77–89. [[CrossRef](#)]
41. Sen, P.K. Estimates of the regression coefficient based on Kendall's Tau. *J. Am. Stat. Assoc.* **1968**, *63*, 1379–1389. [[CrossRef](#)]
42. Park, H.; Jeong, S.J.; Ho, C.H.; Kim, J.; Brown, M.E.; Schaepman, M.E. Nonlinear response of vegetation green-up to local temperature variations in temperate and boreal forests in the Northern Hemisphere. *Remote Sens. Environ.* **2015**, *165*, 100–108. [[CrossRef](#)]
43. Han, X.M.; Zuo, D.P.; Xu, Z.X.; Cai, S.Y.; Gao, X.X. Analysis of vegetation condition and its relationship with meteorological variables in the Yarlung Zangbo River Basin of China. *Proc. Int. Assoc. Hydrol. Sci.* **2018**, *379*, 105–112. [[CrossRef](#)]
44. Li, H.D.; Li, Y.K.; Shen, W.S.; Li, Y.N.; Lin, J.; Lu, X.Y.; Xu, X.; Jiang, J. Elevation-dependent vegetation greening of the Yarlung Zangbo River Basin in the Southern Tibetan Plateau, 1999–2013. *Remote Sens.* **2015**, *7*, 16672–16687. [[CrossRef](#)]
45. Wang, K.; Zhang, L.; Qiu, Y.B.; Ji, L.; Tian, F.; Wang, C.Z.; Wang, Z.Y. Snow effects on alpine vegetation in the Qinghai-Tibetan Plateau. *Int. J. Digit. Earth* **2015**, *8*, 56–73. [[CrossRef](#)]
46. Wan, Y.F.; Gao, Q.Z.; Li, Y.; Qin, X.B.; Ganjurjav, Z.; Zhang, W.N.; Ma, X.; Liu, S. Change of snow cover and its impact on alpine vegetation in the source regions of large rivers on the Qinghai-Tibetan Plateau, China. *Arct. Antarct. Alp. Res.* **2014**, *46*, 632–644. [[CrossRef](#)]

47. Ban, C.; Xu, Z.; Zuo, D.; Zhang, R.; Chen, H.; Ye, C.; Wang, J.; Waciren, D. Impact of variability in the hydrological cycle components on vegetation growth in an alpine basin of the southeastern Tibet Plateau, China. *Hydrol. Res.* **2022**, *53*, 124–140. [[CrossRef](#)]
48. Liu, X.W.; Xu, Z.X.; Liu, W.F.; Liu, L. Responses of hydrological processes to climate change in the Yarlung Zangbo River basin. *Hydrol. Sci. J.* **2019**, *64*, 2057–2067. [[CrossRef](#)]
49. Lu, Y.Y.; Liu, F.; Zhao, Y.G.; Song, X.D.; Zhang, G.L. An integrated method of selecting environmental covariates for predictive soil depth mapping. *J. Integr. Agric.* **2019**, *18*, 301–315. [[CrossRef](#)]
50. Fabris, F.; Doherty, A.; Palmer, D.; de Magalhaes, J.P.; Freitas, A.A. A new approach for interpreting Random Forest models and its application to the biology of ageing. *Bioinformatics* **2018**, *34*, 2449–2456. [[CrossRef](#)] [[PubMed](#)]
51. Li, H.; Liu, L.; Liu, X.; Li, X.; Xu, Z. Greening Implication Inferred from Vegetation Dynamics interacted with climate change and human activities over the Southeast Qinghai–Tibet Plateau. *Remote Sens.* **2019**, *11*, 2421. [[CrossRef](#)]
52. Liu, L.; Niu, Q.; Heng, J.; Li, H.; Xu, Z. Transition characteristics of the Dry-Wet regime and vegetation dynamic responses over the Yarlung Zangbo River Basin, Southeast Qinghai-Tibet Plateau. *Remote Sens.* **2019**, *11*, 1254. [[CrossRef](#)]
53. Filippa, G.; Cremonese, E.; Galvagno, M.; Isabellon, M.; Bayle, A.; Choler, P.; Carlson, B.Z.; Gabellani, S.; di Cella, U.M.; Migliavacca, M. Climatic drivers of greening trends in the Alps. *Remote Sens.* **2019**, *11*, 2527. [[CrossRef](#)]
54. Jiao, K.W.; Gao, J.B.; Wu, S.H.; Hou, W.J. Research progress on the response processes of vegetation activity to climate change. *Acta Ecol. Sin.* **2018**, *38*, 2229–2238.
55. Afuye, G.A.; Kalumba, A.M.; Orimoloye, I.R. Characterisation of vegetation response to climate change: A review. *Sustainability* **2021**, *13*, 7265. [[CrossRef](#)]
56. Zha, X.B.; Luo, P.P.; Zhu, W.; Wang, S.T.; Lyu, J.Q.; Zhou, M.M.; Huo, A.D.; Wang, Z.H. A bibliometric analysis of the research on Sponge City: Current situation and future development direction. *Ecohydrology* **2021**, *14*, e2328. [[CrossRef](#)]
57. Luo, P.P.; Xu, C.Y.; Kang, S.X.; Huo, A.D.; Lyu, J.; Zhou, M.M.; Nover, D. Heavy metals in water and surface sediments of the Fenghe River Basin, China: Assessment and source analysis. *Water Sci. Technol.* **2021**, *84*, 3072–3090. [[CrossRef](#)] [[PubMed](#)]